J. Astrophys. Astr. (1983) **4**, 151–159

Reflection Effect in Close Binaries. III. Distribution of Radiation Incident from an Extended Source

A. Peraiah *Indian Institute of Astrophysics, Bangalore 560034*

Received 1983 January 17; accepted 1983 June 17

Abstract. We have studied the effects of irradiation from an extended surface of the secondary component on the atmosphere of the primary. We have considered an isothermal and purely scattering medium. The resultant radiation field due to irradiation from an extended surface and self-radiation is different from that due to irradiation from a point source and self-radiation. In the case of the point source the middle layers of the exposed part of the atmosphere show maximum reflection while in the former case the reflection gradually decreases from the centre of the component towards the surface of the outermost layers of the atmosphere. The reflection effect appears to be strongly dependent on the density distribution of the electrons.

Key words: reflection effect – radiative transfer – density distribution

1. Introduction

In an earlier paper (Paper 1 in this series) we have investigated the effect of reflection of radiation emitted by the secondary component on the atmosphere of the primary. We have assumed there that the incident radiation is emitted by a point source. This assumption of emission from a point source makes the calculations easy and is a first step towards understanding the effects of reflection. It is found that the maximum emission of the reflected radiation comes from the intermediate points and not from the centre or from the outermost layers of the atmosphere. In reality, we know that the radiation incident on the surface of one component is emitted by an extended surface of the secondary component. This radiation could change the reflected radiation completely and we should hence estimate the latter properly. This is the subject matter of this paper.

2. Computational procedure

The shapes of the components of the system are assumed to be spherical; the incident

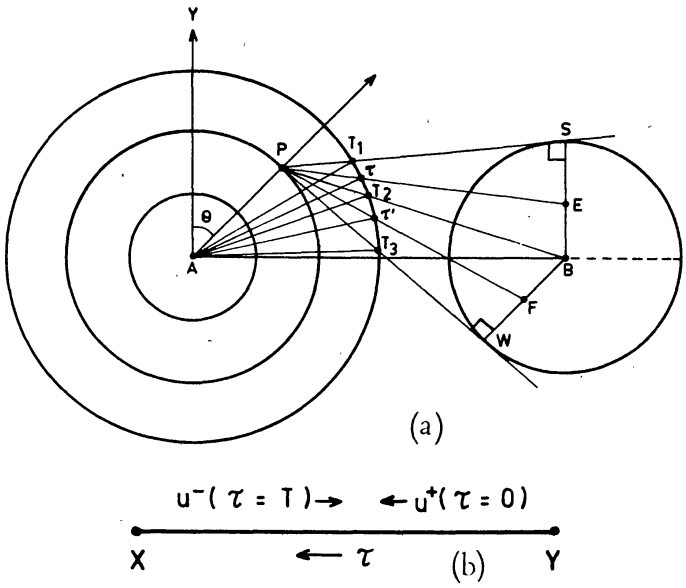

Figure 1. (a) Schematic diagram of the incidence of radiation from an extended surface of the secondary. (b) Schematic diagram of the rod model.

radiation is assumed to come from the spherical surface of the secondary. We divide the atmosphere of the primary into several spherical shells. In Fig. 1(a), we have given the geometrical description of the model. A and B are the centres of the two components separated by a distance AB. The atmosphere of the component with centre at A (which receives radiation from the component whose centre is at B) is divided into several shells. We draw radius vectors which intersect these shells at points such as P. We wish to calculate the distribution of radiation field at such points of intersection. We see that the point P receives radiation emitted by the surface SW of the component whose centre is at B (the sector between tangents PS and PW from the point P to the circle B). We have to calculate the ray paths PT_1, $P\tau$, PT_2, $P\tau'$, PT_3 *etc.*, so that we can calculate the source function at P due to the transfer of radiation along these ray paths. We assume that AP, AB and BS (= BW) are given. $AT_1 = A\tau = \ldots = AT_3$ are the radii of the component which are also assumed to be known. The quantities SE or WE are taken in discrete values to calculate the corresponding ray paths along $P\tau$ *etc.*, inside the atmosphere. The segment $P\tau$ corresponding to SB is given by

$$P\tau = A\tau \frac{\nu}{\Delta} \tag{1}$$

where

$$\nu = \mu'\Delta + \mu\Delta', \quad \mu = \frac{AP}{A\tau}\Delta,$$

$$\mu' = (1-\mu^2)^{\frac{1}{2}}, \quad \Delta = \alpha\beta\gamma + \alpha\beta'\gamma' + \alpha\beta\gamma' - \alpha'\beta'\gamma',$$

$$\Delta' = (1-\Delta^2)^{\frac{1}{2}}, \quad \alpha = \frac{BS}{PB},$$

$$\alpha' = (1-\alpha^2)^{\frac{1}{2}}, \quad \beta' = \frac{AB}{PB}\cos\vartheta,$$

$$\beta' = (1-\beta^2)^{\frac{1}{2}},$$

$$\gamma = \frac{\mathrm{SE}}{\mathrm{PE}}, \quad \gamma' = (1-\gamma^2)^{\frac{1}{2}},$$

$$\mathrm{PB} = (\mathrm{AP}^2 + \mathrm{AB}^2 - 2\mathrm{AP} \times \mathrm{AB} \sin\theta)^{\frac{1}{2}}, \ \mathrm{PE} = (\mathrm{SE}^2 + \mathrm{PS}^2)^{\frac{1}{2}}. \tag{1a}$$

Similarly, the segments $\mathrm{P}\tau'$ corresponding to BW is given by

$$\mathrm{P}\tau' = \mathrm{A}\tau' \frac{e}{c}, \tag{2}$$

where

$$e = cd' + c'd, \quad d = \frac{\mathrm{AP}}{\mathrm{A}\tau'} c,$$

$$d' = (1-d^2)^{\frac{1}{2}}, \quad c = \beta b' - \beta' b,$$

$$c' = (1-c^2)^{\frac{1}{2}}, \quad b = \alpha a' - \alpha' a,$$

$$b' = (1-b^2)^{\frac{1}{2}}, \quad a = \mathrm{WF/PF},$$

$$a' = (1-a^2)^{\frac{1}{2}}. \tag{2a}$$

We shall calculate the specific intensities along the ray paths ($\mathrm{P}\tau$, $\mathrm{P}\tau'$ *etc.*), and estimate the source functions at points such as P. This is done by using the rod model which has been described in Paper 1 (and for details see Grant 1968). The source function at point P in the rod is given by

$$S_{\mathrm{d}}(\tau) = S(\tau) + \tilde{\omega}(\tau)\ P(\tau)\ u_{\mathrm{b}}(\tau), \tag{3}$$

where the second term on the right-hand side is due to the incident radiation and the first term is the contribution to the source due to diffusely-scattered radiation field. The quantity $S(\tau)$ is given by

$$S(\tau) = (1-\tilde{\omega})\ B(\tau) + \tilde{\omega}(\tau)\ P(\tau)\ u(\tau), \tag{4}$$

where $\tilde{\omega}$ is the albedo for single scattering. Furthermore

$$P(\tau) = \begin{bmatrix} p & 1-p \\ 1-p & p \end{bmatrix}, B = \begin{bmatrix} B^+ \\ B^- \end{bmatrix}$$

$$S = \begin{bmatrix} S^+ \\ S^- \end{bmatrix}, \quad u = \begin{bmatrix} u^+ \\ u^- \end{bmatrix}. \tag{5}$$

Here, u^+ and u^- are the specific intensities in the two opposite directions along the segments $\mathrm{P}\tau$ *etc.*, B^+ and B^- are the Planck functions and p is the probability that a photon is scat-

tered in each of the two directions (for isotropic scattering, we set $p = 0.5$); and

$$S^+ = [1 - \tilde{\omega}(\tau)]B^+(\tau) + \tilde{\omega}(\tau)[p(\tau)\ u^+(\tau) + \{1 - p(\tau)\}\ u^-(\tau)],$$

$$S^- = [1 - \tilde{\omega}(\tau)]B^-(\tau) + \tilde{\omega}(\tau)[\{1 - p(\tau)\}u^+(\tau) + p(\tau)u^-(\tau)], \quad (6)$$

with boundary conditions at $\tau = 0$ and at $\tau = T$ (see Fig. 1b); these conditions are written as

$$u^+(0) = u_1 \text{ and } u^-(T) = u_2. \quad (7)$$

The quantity u_b in Equation (3) is given by

$$u_b(\tau) = \begin{bmatrix} u_1 \exp(-\tau) \\ u_2 \exp(T - \tau) \end{bmatrix} \quad (8)$$

We shall specify the quantities u_1 and u_2 in advance. The components of the vector $u_b(\tau)$ express the fact that the intensity at any point and in a given direction results from all the anterior points reduced by $\exp(-\tau)$ of the incident radiation at $\tau = 0$ and by $\exp[-(T - \tau)]$ of the incident radiation at $\tau = T$. In our model, we give the incident radiation at the points T_1, τ *etc.*, and no incident radiation is given at the point P. Therefore we give the boundary condition as

$$u_2 = 0 \quad \text{and} \quad u_1 = I \cos \mu'. \quad (9)$$

I is the ratio of the radiations corresponding to the two components with centres at B and A respectively and μ' is given in Equations (1a). The quantities $u^+(\tau)$ and $u^-(\tau)$ given in Equation (6) are obtained by solving the equations of transfer for the rod given by,

$$\mathbf{M}\frac{d\mathbf{u}}{d\tau} + \mathbf{u} = \mathbf{S}, \quad (10)$$

where

$$\mathbf{M} = \begin{bmatrix} 1 & 0 \\ 0 & -1 \end{bmatrix}. \quad (11)$$

$u^+(\tau)$ and $u^-(\tau)$ are given by

$$u^+(\tau) = u_1 \frac{1 + (T - \tau)\ (1 - p)}{1 + T(1 - p)}, \quad (12)$$

and

$$u^-(\tau) = u_1 \frac{(T - \tau)(1 - p)}{1 + T(1 - p)}, \quad (13)$$

where

$$\tau(X) = \int_0^X N(X')\ \sigma dX' \quad (14)$$

and T is the total optical depth; σ is the electron scattering coefficient and $N(X')$ is the electron density at X' along the raypath. In our case, Equations (12) and (13) are reduced to

$$u^+(\tau = T) = u_1 \frac{1}{1 + T(1-p)} \tag{15}$$

and

$$u^-(\tau = 0) = u_1 \frac{T(1-p)}{1 + T(1-p)}. \tag{16}$$

Using Equations (6) – (16) we can calculate the source function S_d given in Equation (3). The source function due to self-radiation is calculated by solving the equations of transfer in spherical symmetry given by

$$\mu \frac{\partial u(r,\mu)}{\partial r} + \frac{1}{r}\frac{\partial}{\partial \mu}[(1-\mu^2)\, u(r,\mu)] + \sigma(r)\, u(r,\mu)$$
$$= \sigma(r)\{[1-\tilde{\omega}(r)]\, B(r) + \tfrac{1}{2}\tilde{\omega}(r) \int_{-1}^{+1} P(r,\mu,\mu')u(r,\mu')d\mu'\} \tag{17}$$

and

$$-\mu \frac{\partial u(r,-\mu)}{\partial r} - \frac{1}{r}\frac{\partial}{\partial \mu}[(1-\mu^2)\, u(r,-\mu)] + \sigma(r)\, u(r,-\mu)$$
$$= \sigma(r)\{[1-\tilde{\omega}(r)]B(r) + \tfrac{1}{2}\tilde{\omega}(r)\int_{-1}^{+1} P(r,-\mu,\mu')\, u(r,\mu')d\mu'\} \tag{18}$$

where

$$u(r,\mu) = 4\pi r^2\, I(r,\mu), \tag{19}$$

$I(r,\mu)$ is the specific intensity of the ray making an angle of $\cos^{-1}\mu$ with the radius vector at r. $B(r)$ is the Planck function, $P(r,\mu,\mu')$ is the isotropic phase function. $\sigma(r)$ is the absorption coefficient at r. We shall set $\tilde{\omega} = 1$ (for scattering medium) and $B = 0$. In this case the source function due to self-radiation S_S is given by,

$$S_S(r) = \tfrac{1}{2}\int_{-1}^{+1} I(r,\mu)d\mu. \tag{20}$$

The details of obtaining the solution of Equations (17) and (18) are described in Peraiah & Grant (1973). Notice that we have used the specific intensity $I(r,\mu)$ in calculating $S_S(r)$ and not $u(r,\mu)$. The quantity $I(r,\mu)$ defined in Equation (19) is of the same dimension as u^+ or u^- employed in the rod model. We obtain the total source function S_T by adding the source function due to irradiation to that due to self-radiation. From Equation (3) and (20), we have

$$S_T = S_d(r,\tau) + S_S(r). \tag{21}$$

with the help of source function S_T we can estimate the distribution of radiation field at the point P by using the relations (11) and (12) of Paper 1.

3. Results and discussion

The inner radius R_{in} of the component is taken to be equal to 10^{12}cm, the atmosphere is taken to be three times the inner radius ($R_{out} = 3R_{in}$), and the separation of centres AB = $3R_{out}$. We have assumed a purely scattering medium with the electron density changing as r^{-2} in the atmosphere, and taking a value of 10^{13}cm^{-3} at the inner radius R_{in}. The radius of the secondary component is taken to be the same as that of the primary (*i.e.* R_{out}). We have divided the atmosphere into 25 shells (or 26 shell boundaries).

With the above data, the total radial optical depth will be nearly equal to 4. The

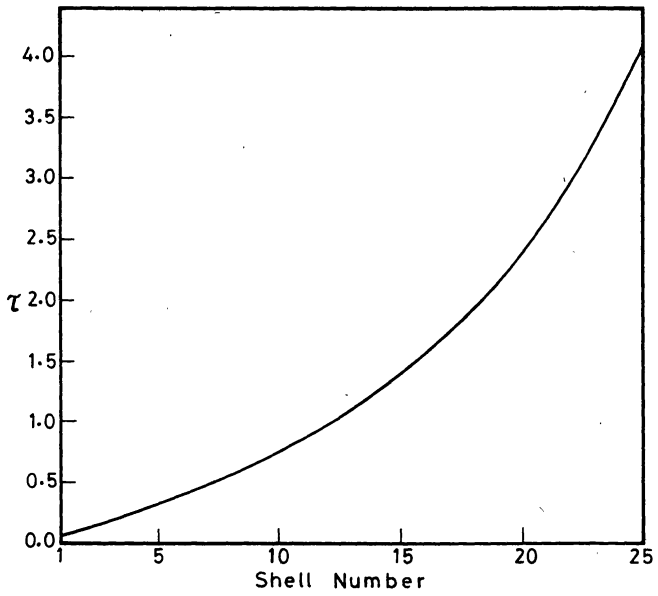

Figure 2. The run of the optical depth with the shell numbers.

optical depths along the segments such as PT *etc.*, change considerably as the rays from the secondary surface are incident at different angles. The optical depth is calculated and is given against the shell numbers in Fig. 2.

Fig. 3 describes the total source functions S_T in each shell. Shell number 1 starts at R_{out} and the boundary of the last shell coincides with the inner radius R_{in}. We have set θ (colatitude) as a free parameter and calculated the radiation field at $\theta = 0°$, 30°, 60° and 90°. In Fig. 3(a), we have shown the total source functions for $I = 1$. We notice that the source function is reduced only slightly and it is almost as much as the incident radiation. The reason for this is that the total source function is the sum of the contributions from the irradiation and self-radiation. If we have only self-radiation then the source function will reduce considerably towards the outer layers of the atmosphere. But the radiation incident from the secondary component enhances the radiation field in the outer layers and raises the value of the source function. At $\theta = 0°$, we notice that the source function falls from $n = 1$ to $n = 26$. This is expected as these source functions are along the axis AY (see Fig. 1a) which is perpendicular to AB. When θ is increased gradually, the source functions increase slowly towards larger values of n. At $\theta = 90°$, the source function increases towards higher values of n. This is because of the direct incidence of the radiation from the secondary component. In Fig. 3(b), we have plotted S_T with respect to the shell numbers for $I = 10$. Except for the fact that the magnitude is enhanced, the nature of variation of S_T is the same as for $I = 1$ for all angles.

Figs 4 and 5 describe the angular distribution of radiation in $-1 \leq \mu \leq 1$ where μ is the cosine of the angle made by the ray with the radius vector at (r,ψ). (for the definition of ψ, see Fig. 3 of paper 1). In Fig. 4(a) the angular distribution of radiation at $n = 1$, 12 and 26 are given for $\theta = 0°$. The continuous lines represent the radiation due to the irradiation from the secondary while the broken lines represent the composite field due to self-radiation of the primary and irradiation due to secondary component. We find that the differences in the fields due to irradiation and total radiation are different at

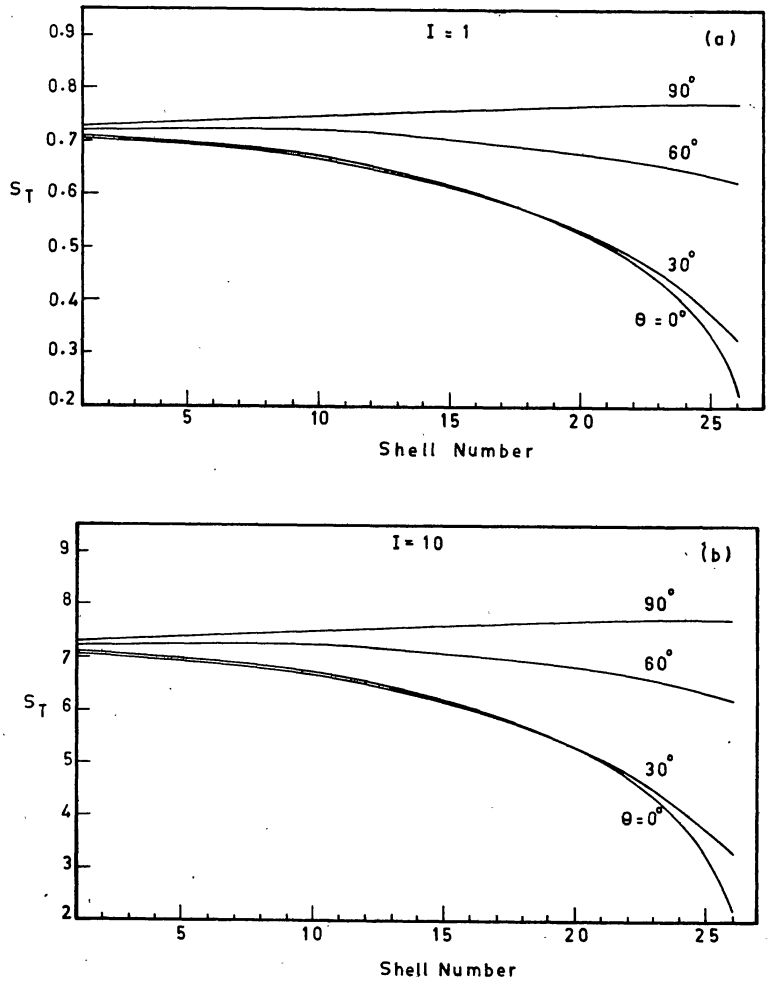

Figure 3. Total source function S_T versus shell numbers for $\theta = 0°$, 30°, 60° and 90°, and (a) $I = 1$, (b) $I = 10$.

different radial points. At the boundary of the shell number 25, the difference is large and this is due to the fact that the self-radiation is dominant and also that the reflected radiation is scattered much more here (because of a higher number of electrons; it can be seen that the optical depth is large at $n = 25$) than at the boundary of the shell number 1. At $n = 1$, we have the intensities reduced considerably because of the fact that the flux in the self-radiation is reduced towards the surface of the atmosphere (at $n = 1$) and there are not sufficient number of electrons to scatter the radiation from the secondary component. In Fig. 4(b), we have shown the angular distribution at $\theta = 90°$. We notice that the same physical characteristics are shown by the curves at both the angles. From $n = 1$ to $n = 25$ we see a gradual increase in the specific intensities of the reflected radiation in both the figures. The optical depth also increases in the same direction. This is because we assumed an increasing density distribution towards the surface of the star. Therefore, one can perhaps interpret the increase of the specific intensities on the basis that there are more electrons scattering the incident radiation as we approach the base of the atmosphere ($n = 25$).

In Fig. 5 we have plotted the angular distribution of the specific intensities for

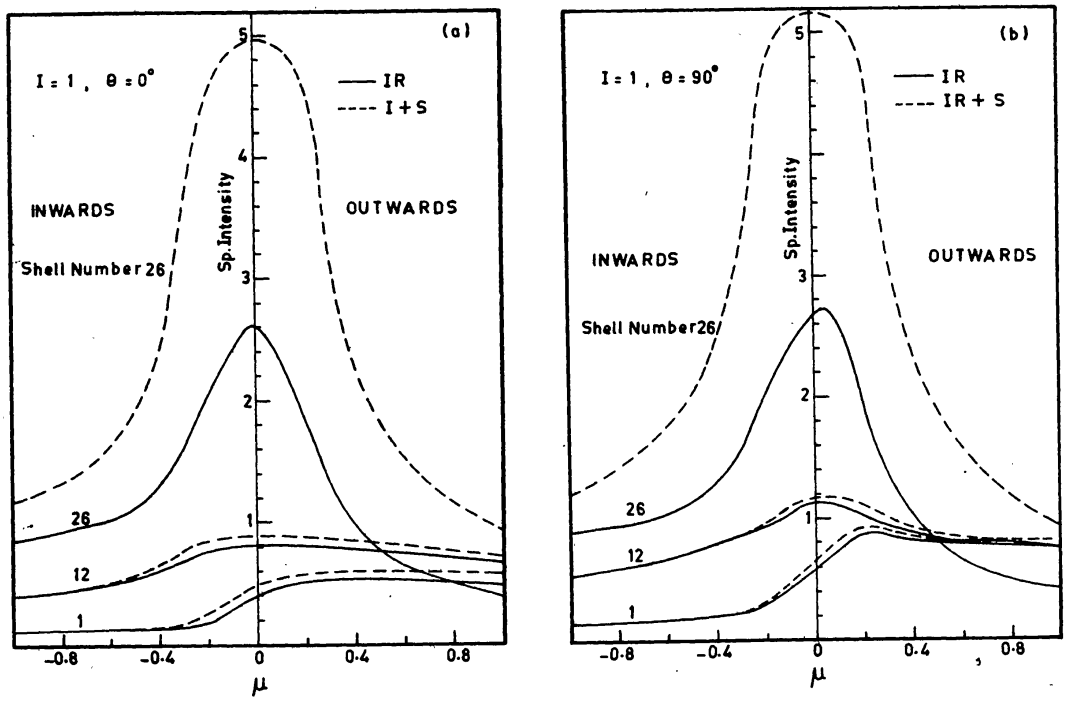

Figure 4. Angular distribution of the radiation field at $I=1$ and (a) $\theta=0°$, (b) $\theta=90°$.

$I=10$, and $\theta=0°$ and 90°. The characteristic changes shown by these curves are similar to those shown in Fig. 4, except that the specific intensities increase because of the increased amount of irradiation from the secondary component.

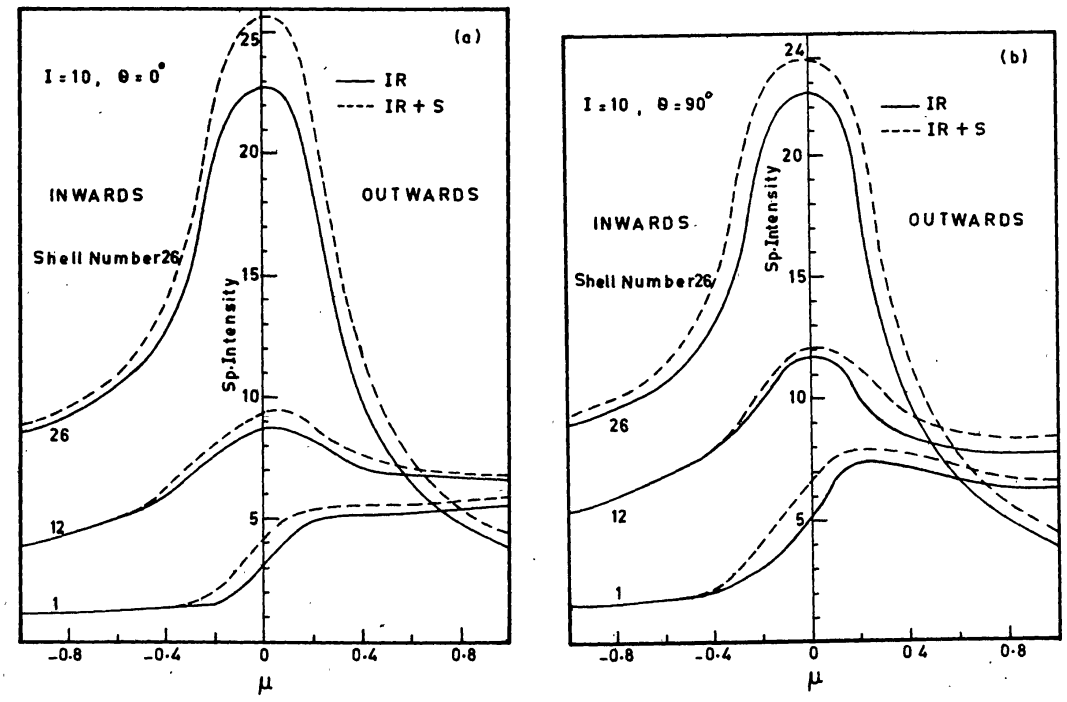

Figure 5. Angular distribution of the radiation field at $I=10$ and (a) $\theta=0°$, (b) $\theta=90°$.

At shell number 25, we notice that the intensities of the inward radiation is higher than those of outward radiation. However, at shell numbers 12 and 1, the situation reverses. This seems to be a common feature at all angles.

In this paper we have investigated the distribution of radiation field due to reflection of the irradiation from an extended surface of the secondary component. We have considered an atmosphere with electron scattering. The results presented here show that the distribution of the reflected radiation field from extended surface of the secondary component is different from that due to irradiation from a point source. In the latter case the middle layers of the exposed part of the atmosphere show maximum illumination while in the former case, the medium is uniformly illuminated, the intensities decreasing from $r = R_{in}$ to $r = R_{out}$.

References

Grant, I.P. 1968, *Lecture Notes on New Methods in Radiative Transfer* (unpublished).

Peraiah, A. 1982, *J.. Astrophys. Astr.*, **3**, 485 (Paper 1).

Peraiah, A., Grant, I. P. 1973, *J. Inst. Math. Appl.*, **12**, 75.